Available at
www.ComputerScienceWeb.com
POWERED BY SCIENCE DIRECT

ELSEVIER

Signal Processing 83 (2003) 1859–1870

SIGNAL PROCESSING

www.elsevier.com/locate/sigpro

A regularized technique for the simultaneous reconstruction of a function and its derivatives with application to nonlinear transistor modeling☆

M. Lázaro , I. Santamaría*, C. Pantaleón , J. Ibáñez , L. Vielva

Departamento Ingeniería de Comunicaciones, ETSIIT, Universidad de Cantabria, Av. Los Castros s/n, 39005 Santander, Spain

Received 8 April 2002; received in revised form 19 March 2003

Abstract

In this paper a new regularized digital filtering technique for the simultaneous approximation of a function and its derivatives is proposed. First, a simple and local method is presented that interpolates the specified sample values exactly. The solution obtained by this method belongs to the space of spline functions, and can be implemented using filter banks. Unfortunately, like most of the methods used to solve interpolation problems using derivatives, it is very sensitive to noise. To overcome this drawback we extend the interpolation method to function approximation by defining a regularized functional, which includes a term forcing the smoothness of the solution. The minimization of this functional is performed by solving a simple linear system of equations or using gradient descent based techniques. The method has been implemented in 1D and 2D input spaces. Some examples show the improved performance of this technique in noisy environments.

Keywords: Regularization; Digital filtering; Derivatives; Interpolation

1. Introduction

The general problem of reconstructing a function, $f(x)$, from a set of its values, $y[n]=f(x[n])$, is a very common problem which has received a great attention in the mathematical literature [21,5], as well as in the signal processing literature [18,6,13].

There exist a number of applications where in addition to a suitable reconstruction of the function it is also necessary to get a close approximation of its derivatives. For instance, the nonlinear modeling of microwave transistors to predict the intermodulation behavior is an example of this problem. In this case, it is necessary to approximate not only the nonlinear current to voltage (I/V) characteristic, but also its derivatives up to the same order of the intermodulation products to be considered [2,11]. Therefore, to predict up to the third order of the intermodulation distortion, which is typical for amplifiers and mixers in applications of communications [12], it is necessary

☆ This work has been supported by the European Community and the Spanish Government through FEDER project 1FD97-1863-C02-01.

* Corresponding author. Tel.: +34-942-201552; fax: +34-942-201488.

E-mail addresses: marce@gtas.dicom.unican.es (M. Lázaro), nacho@gtas.dicom.unican.es (I. Santamaría), carlos@gtas.dicom.unican.es (C. Pantaleón), jesus@gtas.dicom.unican.es (J. Ibáñez), luis@gtas.dicom.unican.es (L. Vielva).

0165-1684/03/$ - see front matter © 2003 Elsevier B.V. All rights reserved.
doi:10.1016/S0165-1684(03)00105-1

to approximate up to the third order derivatives of the I/V characteristic.

Moreover, there exist another kind of applications, such as telemetry or simulation of control of aerial traffic, where the derivatives of the function are easily available and they can be used in the process of function reconstruction. In this case, the information of the derivatives can help to reduce the necessary sampling frequency or to obtain some additional advantages, for example, to improve the immunity against noise.

In all these cases, it is necessary to develop models able to approximate a function and its derivatives from a set of measurements. Several approaches have been proposed in the literature to solve this problem. For example, when the signal is known to be bandlimited, it is possible to use an extension of the Shannon sampling theorem [9,10], which includes the samples of the derivatives in the reconstruction of the function, or the iterative method proposed in [16] for irregular sampling. Recently, a method using perfect reconstruction (PR) filter banks has been proposed [3]. The reconstructed signal belongs to multiresolution spaces and is not bandlimited. An example of this space is the space of spline functions. All these approaches, however, present the drawback of a high sensitivity to noise.

To overcome this drawback, in this paper we propose a new regularized interpolation technique to carry out the simultaneous approximation of a function and its derivatives. The initial interpolation solution belongs to the space of spline functions, and it can be implemented by means of a digital filter bank. Like most of the methods employed to solve interpolation problems using the derivatives, this technique is very sensitive to noise. Therefore, to overcome this drawback, we propose to extend this model to function approximation relaxing the interpolation constraint and imposing additional constraints forcing the smoothness of the solution. This regularized method can help to reduce the degradation in the reconstruction process introduced by the noise in the samples.

The paper is organized as follows. In Section 2 we present the proposed interpolation technique in a 1D input space. In Section 3 the regularized extension of this interpolation technique is presented. The extension of both methods to 2D input spaces is stated in Section 4. Section 5 shows some results obtained with the proposed methods. In Section 6 the regularized method is applied to the large-signal modeling of a MESFET transistor. Finally, in Section 7 the main conclusions are exposed.

2. Local interpolation model (LIM) in 1D input spaces

The general problem we are facing can be stated as follows: given a set of N samples of a function and its first D derivatives

$$y^{d)}[n] = f^{d)}(x[n]), \quad n = \{0, 1, \ldots, N-1\},$$
$$d = \{0, 1, \ldots, D\}, \tag{1}$$

to reconstruct a function $f(x)$, which fulfills the interpolation conditions (1). For the sake of simplicity, uniform sampling, with sampling period T, is considered, i.e. $x[n] = nT$; however, as we will see, the method can be easily extended to nonuniform sampling. Also for simplicity, we will consider here the interpolation problem using only samples of the function and its first derivative ($D = 1$). Moreover, in the sequel the superindex $d = 0$ will be understood.

In this particular case, the goal is to obtain a function in the space of splines of order $D + 1$ (i.e., quadratic splines for $D = 1$) that fulfills the interpolation conditions (1). This quadratic spline, in a 1D input space, can be obtained through a set of synthesis functions obtained using perfect reconstruction filter bank theory [3,20]. Here we describe an alternative formulation, more convenient to the further extension of this interpolation method to a regularized technique for function approximation.

The main idea of the method is to obtain a solution where the derivative is piecewise linear, the interpolation conditions are satisfied, and continuity is assured for both function and derivative. To satisfy these continuity and interpolation constraints, some degrees of freedom must be introduced in the system. An option to introduce them is to add a breakpoint between each two consecutive sampling instants. In this way, the original sequences of samples of the function and its derivative $y^{d)}[n]$ ($d = 0, 1$), can be interpolated by 2 to obtain the interpolated sequences

$$y_i^{d)}[n], \quad d = \{0, 1\}, \quad n = \{0, 1, \ldots, 2N-2\}, \tag{2}$$

where the sampling instants associated with these interpolated sequences are now

$$x_i[n] = \frac{nT}{2}, \quad n = \{0, 1, \ldots, 2N-2\}. \tag{3}$$

Taking into account the continuity and interpolation constraints, and assuming that the derivative is piecewise linear between the interpolation sampling instants, it is possible to obtain the values of function and derivative in the inserted breakpoints. In particular, the interpolated sequences take the following values:

$$y_i^{d)}[2n] = y^{d)}[n], \quad d = \{0, 1\}, \tag{4}$$

$$y_i^{1)}[2n+1] = \frac{2(y[n+1] - y[n])}{T} - \frac{y^{1)}[n] + y^{1)}[n+1]}{2}, \tag{5}$$

$$y_i[2n+1] = \frac{y[n] + y[n+1]}{2} + T\,\frac{(y^{1)}[n] - y^{1)}[n+1])}{8}, \tag{6}$$

where index n in (4) runs from 0 to $N-1$, whereas in (5) and (6) runs from 0 to $N-2$.

Since we know the derivative (the piecewise linear function defined by $y_i^{1)}[n]$), once the interpolated sequences have been obtained, the value of the function can be obtained by integration. Therefore, the reconstructed function $\hat{f}(x)$ at any instant situated between the samples n and $n+1$ of the interpolated sequence, i.e., $x_i[n] \leqslant x < x_i[n+1]$, can be evaluated as

$$\hat{f}(x) = y_i[n] + y_i^{1)}[n]\Delta x + \frac{y_i^{1)}[n+1] - y_i^{1)}[n]}{T}(\Delta x)^2 \tag{7}$$

where $\Delta x = x - x_i[n]$. Let us note that the reconstruction process is completely local: the value of the interpolated sequences in the inserted breakpoints depends on the value of the two samples surrounding it, and the final reconstruction using (7) depends only on the value of the sequences in the extremes of the interval. The advantage of this fact is two-fold: in one hand, a low computational burden to carry out the reconstruction and, in the other hand, the method can be immediately extended to nonuniform sampling. Because of this locality we have called this method the local interpolation method (LIM).

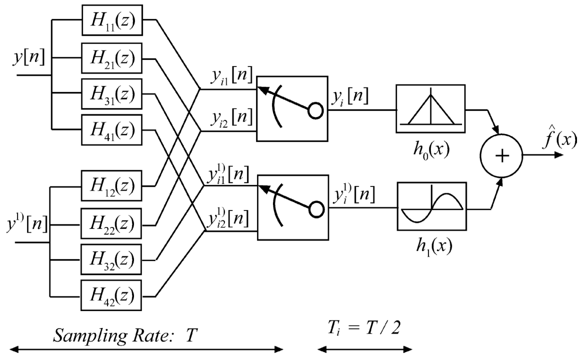

Fig. 1. MIMO filter bank representation of LMI for $D = 1$.

In order to facilitate the notation for the extension to a 2D input space, we will use the following notation to denote the 1D reconstruction procedure of the LIM:

$$\hat{f}(x) = \mathrm{LIM}_{1\mathrm{D}}(y[n], y^{1)}[n]). \tag{8}$$

2.1. Filter bank representation of the interpolation procedure

The interpolation procedure described above admits a representation by means of a multiple input multiple output (MIMO) digital filter bank, followed by a set of analog filters for the reconstruction. Fig. 1 shows this filter bank representation for $D = 1$.

The MIMO digital filter bank performs the interpolation of the sequences of samples by means of polyphase filters. We have denoted $y_{ij}^{d)}[n]$ as the jth polyphase component of the interpolated sequence $y_i^{d)}[n]$. From these polyphase components, the interpolated sequences $y_i[n]$ and $y_i^{1)}[n]$ are obtained. Each interpolated sequence is then filtered by an analog reconstruction filter and both outputs are added to obtain the reconstructed function $\hat{f}(x)$.

The response of the MIMO polyphase filters can be easily obtained from expressions (4)–(6)

$$H_{11}(z) = H_{32}(z) = 1, \quad H_{12}(z) = H_{31}(z) = 0,$$

$$H_{21}(z) = \frac{z+1}{2}, \quad H_{41}(z) = \frac{2z-2}{T},$$

$$H_{22}(z) = \frac{1-z}{8}\,T, \quad H_{42}(z) = -\frac{z+1}{2}. \tag{9}$$

The continuous-time reconstruction filters have the following impulsive responses:

$$h_0(x) = 1 - \frac{|x|}{T_i}, \quad \text{for } |x| \leqslant T_i \tag{10}$$

and

$$h_1(x) = \frac{x}{2}\left(1 - \frac{|x|}{T_i}\right), \quad \text{for } |x| \leqslant T_i, \tag{11}$$

where T_i is the sampling period associated to the interpolated sequences $y_i^{d)}[n]$, i.e, $T_i = T/2$.

The corresponding frequency responses are

$$H_0(\Omega) = T_i \operatorname{sinc}^2\left(\frac{\Omega T_i}{2\pi}\right), \tag{12}$$

and

$$H_1(\Omega) = -\frac{2j}{\Omega^3 T_i}\left(2\sin^2\left(\frac{\Omega T_i}{2}\right) - \Omega T_i \cos\left(\frac{\Omega T_i}{2}\right)\sin\left(\frac{\Omega T_i}{2}\right)\right). \tag{13}$$

It can be seen that this method uses only FIR filters, which makes possible to obtain a local reconstruction, as opposed to the conventional spline techniques, based on IIR filtering [19].

The extension of this model to D derivatives is based on the same idea expressed for $D = 1$. In this case, it is necessary to insert D new breakpoints between consecutive sampling instants in each sequence of samples and the derivative of order D is assumed piecewise linear. Therefore, the initial sequences are interpolated by a factor $D + 1$, and the corresponding solution belongs to the space of splines of degree $D+1$. For example, for 2 derivatives, the solution belongs to the space of cubic splines. The expressions of the polyphase and analog reconstruction filters for 2 derivatives can be found in Appendix A, and an extension to 3 derivatives can be found in [7].

2.2. Noise sensitivity analysis

In this section we analyze the degradation caused by the measurement noise in the interpolation procedure. We assume that the noise in the function and its derivatives can be modeled as a zero-mean white Gaussian noise with variances σ_0^2 and σ_1^2, respectively. Then, taking into account Eq. (4)–(7), it is easy to obtain the noise variance at any point of the reconstructed signals. Specifically, for $0 \leqslant x \leqslant T/2$, the noise variance in the reconstructed function $\sigma_{0r}^2(x)$ and its derivative $\sigma_{1r}^2(x)$ are given by

$$\sigma_{0r}^2(x) = \sigma_0^2\left[\left(1 - \frac{2x^2}{T^2}\right)^2 + \frac{4x^4}{T^4}\right] + \sigma_1^2\left[\left(1 - \frac{3x^2}{2T}\right)^2 + \frac{x^4}{4T^2}\right], \tag{14}$$

$$\sigma_{1r}^2(x) = \sigma_1^2\left[\left(1 - \frac{3x}{T}\right)^2 + \frac{x^2}{T^2}\right] + \frac{32x^2}{T^4}\sigma_0^2. \tag{15}$$

The interesting point is that the noise variance for the derivative, $\sigma_{1r}^2(x)$, varies as $32\sigma_0^2 x^2/T^4$. For instance, at $x = T/2$, the noise variance in the reconstructed derivative depends on $8\sigma_0^2/T^2$. This points out the noise sensitivity of this method, mainly when the signals are oversampled. This noise sensitivity is shared by all the methods usually employed to solve this interpolation problem, and it is the main reason to search for a regularization procedure.

3. Local regularized model

When the measurements are corrupted with noise, instead of requiring an exact interpolation, a more convenient alternative is to relax the interpolation constraints and to force some degree of smoothness in the solution. This can be achieved by minimizing a regularization functional as

$$J(y_r^{d)}) = \sum_{d=0}^{D}\left(\lambda_d \sum_{n=0}^{N-1}(y_r^{d)}[n] - y^{d)}[n])^2\right) + \lambda_r J_r(y_r^{d)}[n]), \tag{16}$$

where $y_r^{d)}[n]$ are the sequences of regularized samples, which now do not fulfill the interpolation conditions, i.e., now in general $y_r^{d)}[n] \neq f^{d)}(x[n])$. The first term measures the error of the solution with respect to the measurements, and the second one is a regularization term that measures the smoothness of the solution. The parameters λ_d y λ_r weight the contribution of the error of the dth order derivative and the regularization term, respectively.

Here we will use a usual measure of smoothness, which is the squared second derivative of the solution. For the particular case we are dealing with (function+first derivative, i.e., $D=1$), it takes the value

$$J_r = \sum_{n=0}^{2N-3} (y_i^{1)}[n] - y_i^{1)}[n+1])^2. \tag{17}$$

where the sequence $y_i^{1)}[n]$ is again the interpolated sequence of the derivative. Similarly to (4) and (5), this sequence can be written as a function of the regularized sequences as

$$y_i^{1)}[2n] = y_r^{1)}[n], \quad n = 0, \ldots, N-1, \tag{18}$$

and

$$y_i^{1)}[2n+1] = \frac{2(y_r[n+1] - y_r[n])}{T} - \frac{y_r^{1)}[n] + y_r^{1)}[n+1]}{2}, \tag{19}$$

where $n=0,1,\ldots,N-2$. Therefore, substituting (18) and (19) into (17), we see that the functional (16) only depends on the regularized sequences $y_r^{d)}[n]$. To obtain the minimum of this functional we evaluate its derivatives with respect to the components of the regularized sequences $y_r^{d)}[n]$

$$\frac{\partial J}{\partial y_r[n]} = 2\lambda_0(y_r[n] - y[n]) + \lambda_r \frac{\partial J_r}{\partial y_r[n]}, \tag{20}$$

$$\frac{\partial J}{\partial y_r^{1)}[n]} = 2\lambda_1(y_r^{1)}[n] - y^{1)}[n]) + \lambda_r \frac{\partial J_r}{\partial y_r^{1)}[n]}. \tag{21}$$

Taking into account (17)–(19) it can be seen that for $n=0$

$$\begin{aligned} \frac{\partial J_r}{\partial y_r[n]} &= \frac{16}{T^2}(y_r[n] - y_r[n+1]) \\ &\quad + \frac{8}{T}(y_r^{1)}[n] + y_r^{1)}[n+1]), \\ \frac{\partial J_r}{\partial y_r^{1)}[n]} &= \frac{8}{T}(y_r[n] - y_r[n+1]) \\ &\quad + 5y_r^{1)}[n] + 3y_r^{1)}[n+1], \end{aligned} \tag{22}$$

whereas for $0 < n < N-1$

$$\begin{aligned} \frac{\partial J_r}{\partial y_r[n]} &= \frac{16}{T^2}(2y_r[n] - y_r[n-1] - y_r[n+1]) \\ &\quad + \frac{8}{T}(y_r^{1)}[n+1] - y_r^{1)}[n-1]), \\ \frac{\partial J_r}{\partial y_r^{1)}[n]} &= \frac{8}{T}(2y_r[n-1] - y_r[n+1]) + 10y_r^{1)}[n] \\ &\quad + 3y_r^{1)}[n+1] + 3y_r^{1)}[n-1]), \end{aligned} \tag{23}$$

and, finally, for $n = N-1$

$$\begin{aligned} \frac{\partial J_r}{\partial y_r[n]} &= \frac{16}{T^2}(y_r[n] - y_r[n-1]) \\ &\quad - \frac{8}{T}(y_r^{1)}[n] + y_r^{1)}[n-1]), \\ \frac{\partial J_r}{\partial y_r^{1)}[n]} &= \frac{8}{T}(y_r[n-1] - y_r[n]) \\ &\quad + 5y_r^{1)}[n] + 3y_r^{1)}[n-1]. \end{aligned} \tag{24}$$

Equating the derivatives (20) and (21) to zero, we obtain a linear system of equations, which can be expressed as

$$\mathbf{b} = \mathbf{A}\mathbf{x}, \tag{25}$$

where

$$\begin{aligned} \mathbf{b} = [&\lambda_0(x[0], \ldots, x[N-1]), \\ &\lambda_1(x^{1)}[0], \ldots, x^{1)}[N-1])]^{\mathrm{T}}, \end{aligned} \tag{26}$$

$$\begin{aligned} \mathbf{x} = [&x_r[0], \ldots, x_r[N-1], \\ &x_r^{1)}[0], \ldots, x_r^{1)}[N-1]]^{\mathrm{T}}, \end{aligned} \tag{27}$$

and $\mathbf{A}$ is a $(2N \times 2N)$ matrix. Typically rank $(\mathbf{A})=2N$, and therefore the solution can be obtained as

$$\mathbf{x} = \mathbf{A}^{-1}\mathbf{b}. \tag{28}$$

Eq. (28) provides the regularized solution; however matrix inversion can be computationally expensive when the number of samples N is high. In this case, the problem can be solved more efficiently by using an iterative gradient-based algorithm. It is important to notice the local behavior of expressions (22)–(24), which makes the computational burden of the gradient-based approach to grow only linearly with N.

Once the regularized sequences have been obtained, the function is reconstructed by using the interpolation model described in Section 2

$$\hat{f}(x) = \mathrm{LIM}_{1D}(y_r[n], y_r^{1)}[n]). \tag{29}$$

The extension to D derivatives follows the same idea. The corresponding expressions can be found in [7].

3.1. Selection of regularization parameters

A very important aspect of this regularization method is the selection of the weight parameters λ_d ($d = 0, 1, \ldots, D$) and the regularization parameter λ_r. There exist several alternatives for this selection. If there is not any knowledge about the noise power in the samples of the function, (σ_0^2), and of the derivatives, (σ_d^2), we should fix the values of λ_d and then select λ_r employing cross-validation techniques [15,17]. To estimate the values of λ_d we propose to select $\lambda_0 = 1$, and then select the rest of values to consider the energy of the different derivatives with respect to the function.

When it is possible to estimate the noise variances, a simple alternative that provides suitable results is to fix $\lambda_0 = 1$ and then select

$$\lambda_d = \frac{\sigma_0^2}{\sigma_d^2} \tag{30}$$

and

$$\lambda_r = \frac{P_0}{P_1^2}\frac{\sigma_0^2}{T^2}, \tag{31}$$

where P_0 and P_1 are the power of the function and the derivative, respectively, which can be easily estimated. We want to remark that this expression is generic, valid for any value of D.

4. Extension to 2D input spaces

In this section we present the extension of the LIM and LRM models to 2D input spaces.

4.1. Local interpolation model

The problem can be stated as follows: given a set of samples of a function, $f(x_1, x_2)$, and of its derivatives

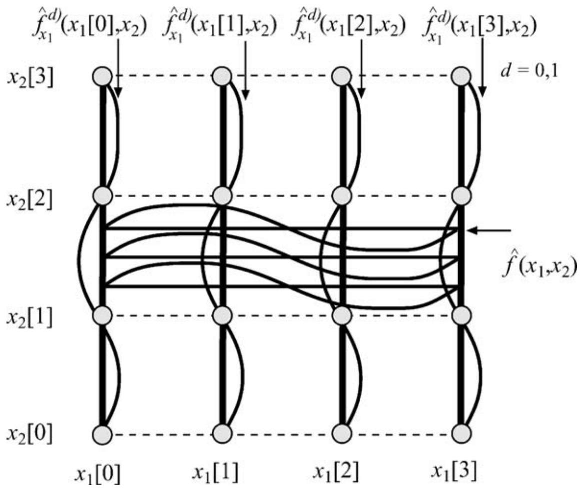

Fig. 2. 2D reconstruction scheme.

up to the order D as

$$y_{x_1,x_2}^{(d_1,d_2)}[n_1,n_2] = \left.\frac{\partial^{(d_1+d_2)} f(x_1,x_2)}{\partial x_1^{d_1}\,\partial x_2^{d_2}}\right|_{x_1=x_1[n_1];x_2=x_2[n_2]}, \tag{32}$$

with $d_1 = 0, \ldots, D$, and $d_2 = 0, \ldots, D$, and where

$$x[n_k] = n_k T_k, \quad k = 1, 2; \quad n_k = 0, \ldots, N_k - 1, \tag{33}$$

being T_k the sampling period in the kth direction of the input space, the objective is to find a function, $\hat{f}(x_1, x_2)$, which interpolates the samples (32) of the function $f(x_1, x_2)$ and its derivatives.

The problem is restricted to the particular case of uniform sampling over a grid of $N_1 \times N_2$ sampling instants. Again, for the sake of simplicity, we consider the case $D = 1$. In this case, to simplify the notation, the superindexes will be understood in (32). We have a set of samples of the function, $y[n_1, n_2]$, of its first derivatives with respect to x_1 and x_2, $y_{x_1}[n_1, n_2]$ and $y_{x_2}[n_1, n_2]$, and of the crossed derivative with respect to both variables, $y_{x_1,x_2}[n_1, n_2]$.

The proposed interpolation method is based on the 1D model presented in Section 2. The reconstruction process is illustrated in Fig. 2.

A direction of reconstruction, x_1 in this case (horizontal lines), is selected and then the LIM_{1D} model is applied in this direction to carry out the function reconstruction. The reconstruction is performed in terms of the function and the derivative with respect to the reconstruction direction, x_1. Therefore, we need to know the value of these two functions in the sampling instants $x_1[n]$ for any x_2 (vertical lines in the figure). Specifically, from the knowledge of

$$\hat{f}(x_1[n_1], x_2), \tag{34}$$

and

$$\hat{f}_{x_1}(x_1[n_1], x_2), \tag{35}$$

the reconstruction of $\hat{f}(x_1, x_2)$, for any value of x_2, is reduced to a 1D problem in the direction x_1.

To reconstruct (34) and (35) the $\mathrm{LIM}_{1\mathrm{D}}$ model, in the direction of x_2, is employed. In this case, each function and its derivative with respect to x_2 are the arguments of the model

$$\hat{f}(x_1[n_1], x_2) = \mathrm{LIM}_{1\mathrm{D}}(y[n_1, n], y_{x_2}[n_1, n]), \tag{36}$$

and

$$\hat{f}_{x_1}(x_1[n_1], x_2) = \mathrm{LIM}_{1\mathrm{D}}(y_{x_1}[n_1, n], y_{x_1,x_2}[n_1, n]). \tag{37}$$

Finally, the function is reconstructed by using the $\mathrm{LIM}_{1\mathrm{D}}$ model in the direction x_1

$$\hat{f}(x_1, x_2) = \mathrm{LIM}_{1\mathrm{D}}(\hat{f}(x_1[n_1], x_2), \hat{f}_{x_1}(x_1[n_1], x_2)). \tag{38}$$

The obtained solution is independent of the selected direction of reconstruction: the same result is obtained if we select x_2 to carry out the reconstruction.

4.2. Regularized model

Again, as in the 1D case, the interpolation model presents high-noise sensitivity. Therefore, it is convenient to regularize the samples in order to reduce this sensitivity. In this case, the following 2D regularization functional is employed:

$$J_r = \int_R \left[\left(\frac{\partial^2 \hat{f}(x_1, x_2)}{\partial x_1^2} \right)^2 + 2 \left(\frac{\partial^2 \hat{f}(x_1, x_2)}{\partial x_1 \partial x_2} \right)^2 + \left(\frac{\partial^2 \hat{f}(x_1, x_2)}{\partial x_2^2} \right)^2 \right] \mathrm{d}x_1 \, \mathrm{d}x_2, \tag{39}$$

where R is the integration domain. In this case, it is the rectangle defined by the sampling instants. Like in the 1D case, the whole regularization functional, J, consists of a weighted sum of the quadratic errors in the samples of the function and its derivatives and the term of regularization J_r. For $D = 1$ this functional is

$$\begin{aligned} J = {} & \lambda_0 \sum_{n_1=0}^{N_1-1} \sum_{n_2=0}^{N_2-1} (y_r[n_1, n_2] - y[n_1, n_2])^2 \\ & + \lambda_1 \sum_{n_1=0}^{N_1-1} \sum_{n_2=0}^{N_2-1} (y_{x_1 r}[n_1, n_2] - y_{x_1}[n_1, n_2])^2 \\ & + \lambda_2 \sum_{n_1=0}^{N_1-1} \sum_{n_2=0}^{N_2-1} (y_{x_2 r}[n_1, n_2] - y_{x_2}[n_1, n_2])^2 \\ & + \lambda_{1,2} \sum_{n_1=0}^{N_1-1} \sum_{n_2=0}^{N_2-1} (y_{x_1, x_2 r}[n_1, n_2] - y_{x_1, x_2}[n_1, n_2])^2 \\ & + \lambda_r J_r, \end{aligned} \tag{40}$$

where $y_r[n_1, n_2]$, $y_{x_1 r}[n_1, n_2]$, $y_{x_2 r}[n_1, n_2]$ and $y_{x_1, x_2 r}[n_1, n_2]$, are the regularized samples of the function, derivative with respect to x_1, derivative, with respect to x_2, and the crossed derivative, respectively.

Taking the derivative of J with respect to the regularized samples and equating to zero the corresponding equations, a matrix system, similar to (25), is obtained. The regularized samples are applied to the interpolation model to perform the reconstruction.

The regularization parameters λ_d are obtained as in the 1D case by (30). The λ_r is obtained as the mean value obtained after applying (31) independently for the first derivatives with respect to x_1 and x_2.

5. Results

Preliminary results for 1D input spaces are available in [8]. In this section, we provide new results obtained in 1D input spaces, and results for 2D input spaces.

5.1. Results in a 1D input space

In this case, the test functions are bandlimited signals generated as a linear combination of 100 sinusoids with random amplitudes, variances and phases.

Fig. 3 compares the reconstruction of a signal limited to the band of 0.1 Hz, with a sampling period $T = 1$, carried out with the LIM and the LRM models for $D = 2$ derivatives. The signal-to-error ratio (SNR) of the samples of function and derivatives is 20 dB.

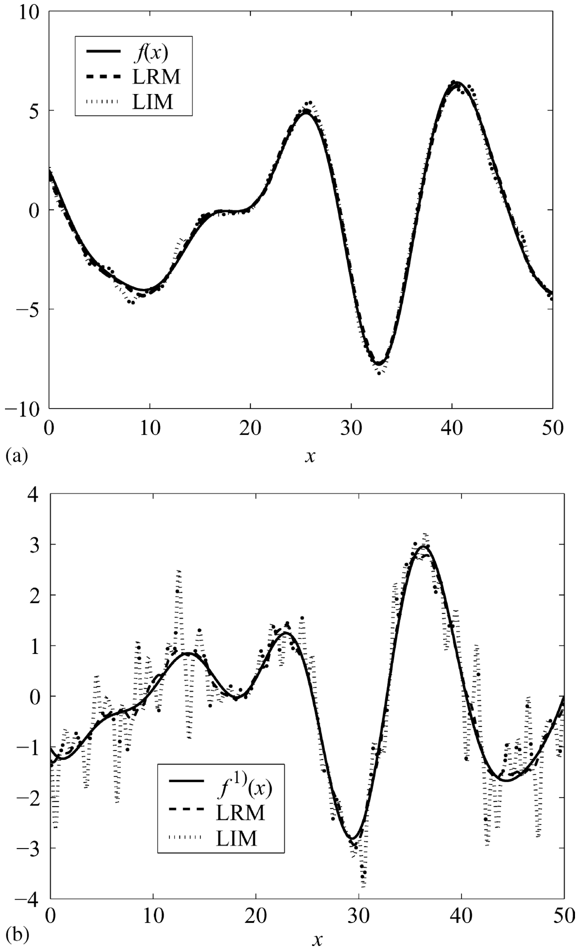

Fig. 3. Reconstruction of a bandlimited signal with the LIM and LRM models. (a) Reconstruction of the function. (b) Reconstruction of the derivative.

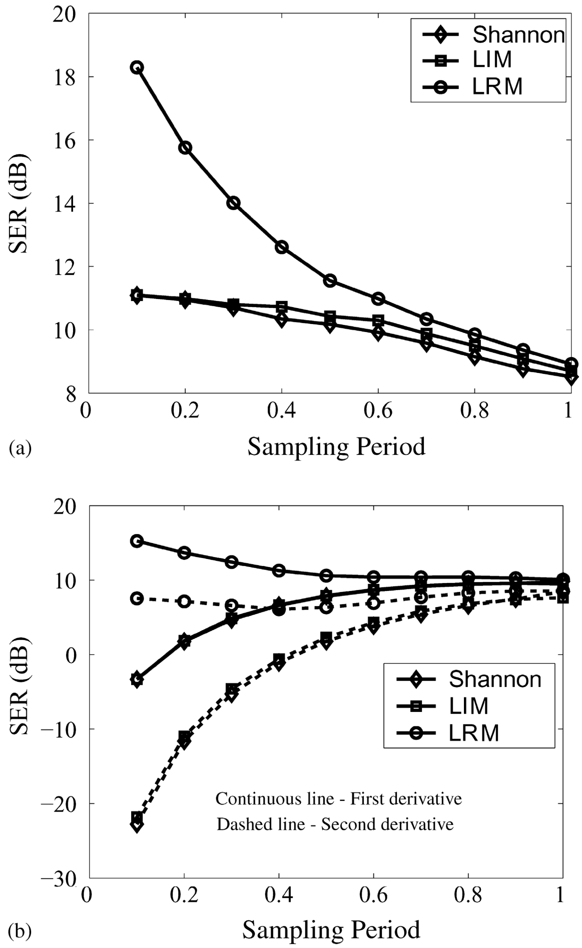

Fig. 4. Reconstruction of function with bandwith 1, with a SNR of 10 dB in the samples of the function and of the derivatives as a function of the sampling rate.

It can be seen that the reconstruction using the LRM is considerably better than that obtained with the LIM, specially in the reconstruction of the derivative. This case corresponds to a highly oversampled signal, when the noise sensitivity of the LIM is high.

Now we compare the performance of the LRM, for $D = 2$, with the LIM and with the extension of the Shannon Sampling Theorem to the sampling of the derivatives [9,10]. Fig. 4 shows the results obtained in the reconstruction of a function of unity bandwidth, with a SNR in the samples of function and derivatives of 10 dB, as a function of the sampling period. The results of 1000 experiments have been averaged.

The LRM provides better results than the LIM and the Shannon method, specially in the reconstruction of the derivatives. We can see that, when T decreases, the interpolation methods suffer a high degradation in the reconstruction of the derivatives, while the LRM does not present such a degradation.

5.2. Results in a 2D input space

For the 2D input space, we have selected as test functions the set of 8 functions used in [1] to perform a comparison of several adaptive methods for function estimation. These functions are presented in Table 1.

Table 1
Functions used to generate the 2D data sets

Name	Function	Domain
Fun 1	$y = \sin(x_1 x_2)$	$[-2, 2]$
Fun 2	$y = \exp(x_1 \sin(\pi x_2))$	$[-1, 1]$
Fun 3	$y = \frac{40\exp(8((x_1-0.5)^2+(x_2-0.5)^2))}{\exp(8((x_1-0.2)^2+(x_2-0.7)^2))+\exp(8((x_1-0.7^2)+(x_2-0.2)^2))}$	[0,1]
Fun 4	$y = (1+\sin(2x_1+3x_2))/(3.5+\sin(x_1-x_2))$	$[-2, 2]$
Fun 5	$y = 42.659(0.1 + x_1(0.05 + x_1^4 - 10x_1^2x_2^2 + 5x_2^4))$	$[-0.5, 0.5]$
Fun 6	$y = 1.3356[1.5(1-x_1) + \exp(2x_1-1)\sin(3\pi(x_1-0.6)^2)$ $+\exp(3(x_2-0.5))\sin(4\pi(x_2-0.9)^2)]$	[0,1]
Fun 7	$y = 1.9[1.35 + \exp(x_1)\sin(13(x_1-0.6)^2)$ $+\exp(3(x_2-0.5))\sin(4\pi(x_2-0.9)^2)]$	[0,1]
Fun 8	$y = \sin(2\pi\sqrt{x_1^2+x_2^2})$	$[-1, 1]$

Table 2
Results (SER in dB) of the approximation for the different test functions and its derivatives with the LIM and LRM models taking 15 equidistant sampling points in each axis of the input space. Results are provided individually for each of the 8 test functions (columns "Fun 1" to "Fun 8") and the mean value over the 8 test functions (column "Mean"). For the first and second order derivatives, the mean SER value of the derivatives with respect to each direction of the input space is presented

	Fun 1	Fun 2	Fun 3	Fun 4	Fun 5	Fun 6	Fun 7	Fun 8	Mean
Approximation of the function									
LIM	21.7	21.5	21.6	21.6	19.9	21.5	21.7	21.4	21.3
LRM	32.2	29.5	35.3	20.9	31.7	27.5	30.2	27.1	29.3
Approximation of the first-order derivatives									
LIM	7.1	6.5	3.5	12.1	9.4	8.9	9.4	11.4	8.5
LRM	24.8	23.0	21.3	18.9	24.7	22.3	20.9	18.9	21.9
Approximation of the second-order derivatives									
LIM	−12.3	−18.3	−17.1	−3.3	−8.1	−5.7	−5.6	−3.4	−9.2
LRM	9.2	−1.5	1.6	8.8	14.7	16.4	7.5	7.0	8.0

In this case, the behavior is similar to the 1D case. Table 2 compares the results, expressed by the SER in dB, obtained reconstructing the test functions with the LIM and the LRM. In this case, a grid of 15×15 equidistant sampling instants have been used, obtaining 225 sampling instants. The results presented for the first and second order derivatives correspond to the mean value of the derivatives with respect to both directions of the input space. It can be seen that the regularized solution provides better results than the interpolated one. Again, the LRM avoids the high degradation in the reconstruction of the derivatives that the interpolation method exhibits.

6. Large-signal modeling of a MESFET transistor

As it was said in the introduction, the modeling of microwave transistors is an example of application where the reconstruction of the derivatives is

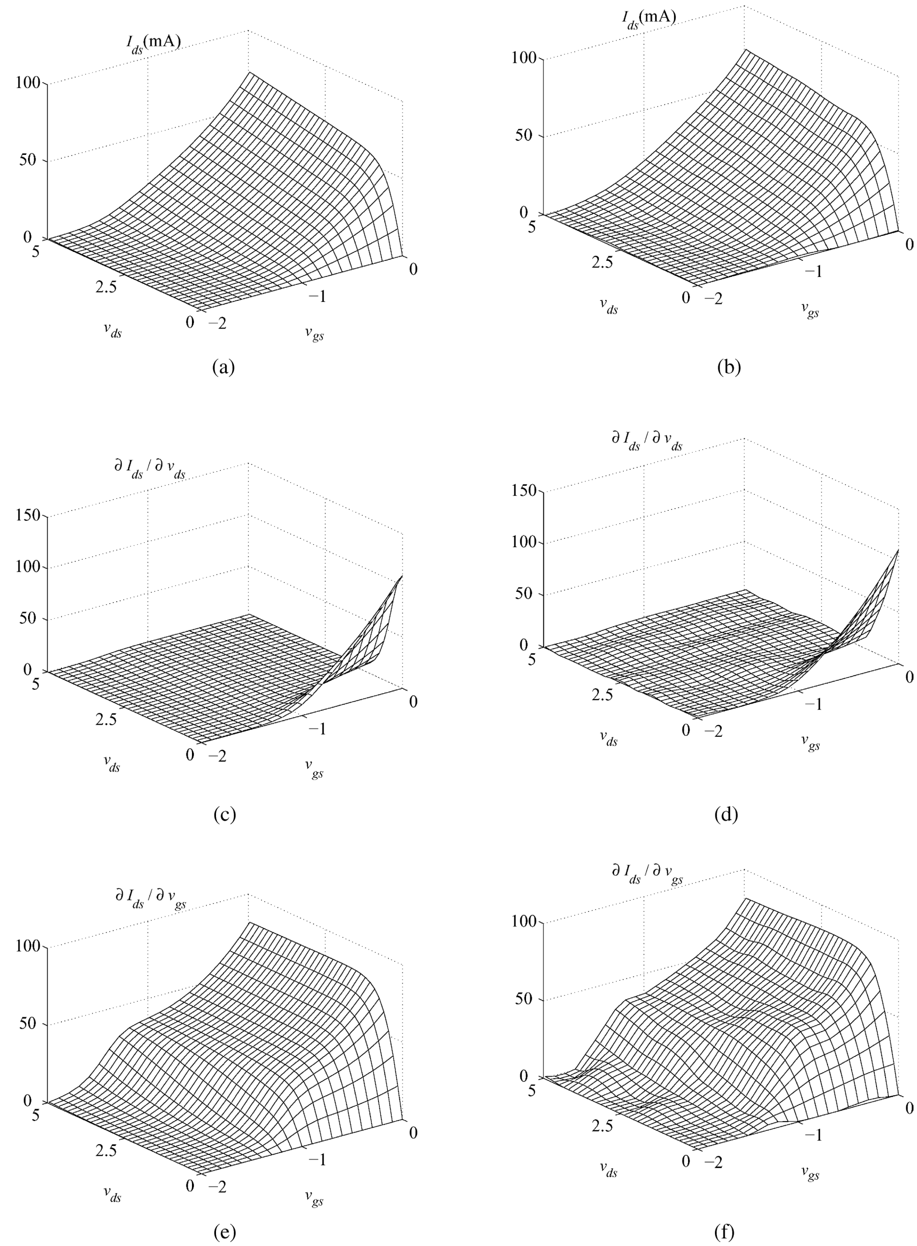

Fig. 5. I/V characteristic and its derivatives vs. the approximation obtained with the LMR model. Measurements (a), (c) and (e) vs. approximation (b), (d) and (f).

relevant, specially when the intermodulation distortion must be taken into account. Here, we propose to use the LRM to obtain a large-signal model of a MESFET, for a given bias point (V_{ds0}, V_{gs0}), from a set of measurements of the drain to source current, I_{ds}, and its derivatives for different values of the dynamic voltages v_{ds} and v_{gs}. It is known that the large-signal behavior of a MESFET transistor is governed by the dynamic pulsed I/V characteristic that depends on the quiescent bias point [4]. The approximation of the derivatives

Table 3
Results of the reconstruction of I_{ds} and its derivatives for a MESFET NE72084

I_{ds}	$\frac{\partial I_{ds}}{\partial v_{ds}}$	$\frac{\partial I_{ds}}{\partial v_{gs}}$	$\frac{\partial^2 I_{ds}}{\partial v_{ds} v_{gs}}$
30.2 dB	21.3 dB	23.5 dB	15.9 dB

of this characteristic can improve the reproduction of the whole behavior of the device.

In this case, we have used the LRM of degree 2 to model a MESFET NE72084. The set of measurements has been obtained from an analytic model of this transistor [14].

Fig. 5 compares the measurements and the approximation provided by the LRM for the bias point $V_{ds0} = 4$ V ans $V_{gs0} = -1$ V. A set of 25 measurements (in a grid of 5×5 equidistant sampling instants) of I_{ds} and its derivatives with respect to v_{ds}, to v_{gs} and the crossed derivative with respect to the both variables has been used, giving a complete set of 100 measures for bias point. A SNR of 30 dB has been considered for all measures.

It can be seen that the LRM model provides a suitable approximation of the set of measures. Table 3 shows the SER of the reconstruction of I_{ds} and its derivatives.

7. Conclusions

In this paper a new interpolation technique for the simultaneous reconstruction of a function and its derivatives has been presented. The reconstruction process can be implemented by means of an FIR filter bank. In a 1D input space, this approach provides the same solution that that proposed in [3,20]. Here, the method has been extended to 2D input spaces.

Because of the noise sensitivity of the interpolation approach, a regularized solution has been proposed. This approach improves the performance of the reconstruction process in noisy environments. The sensitivity is more important as the sampling rate increases and, therefore, the improvement of the regularized solution is higher in this case.

Experimental results have shown the advantage of regularization in noisy environments, both in 1D and 2D input spaces. Moreover, the proposed regularization technique has been applied to the nonlinear modeling of a MESFET transistor.

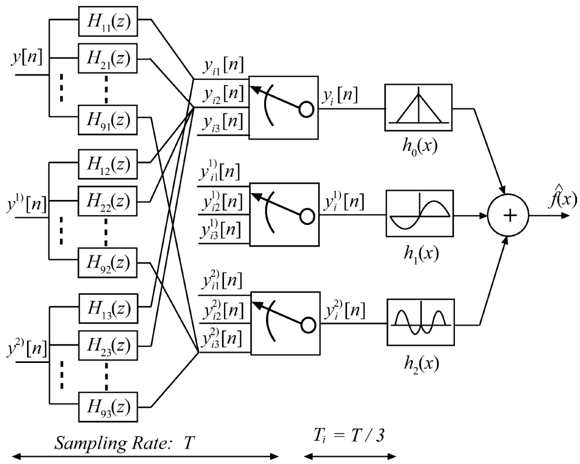

Fig. 6. MIMO filter bank representation of LMI for $D = 2$.

Appendix A

This appendix shows the expressions of the polyphase and analog reconstruction filters for 2 derivatives.

A.1. Polyphase filters for 2 derivatives

The MIMO filter bank for 2 derivatives is shown in Fig. 6.

In this case, the following polyphase filters are necessary:

H_{xy},

with $x = 1,\ldots,9$ and $y = 1,\ldots,3$. These filters take the following values:

$$H_{11}(z) = H_{42}(z) = H_{73} = 1;$$

$$H_{12}(z) = H_{13}(z) = H_{41}(z) = H_{43}(z)$$
$$= H_{71}(z) = H_{72}(z) = 0;$$

$$H_{21}(z) = \frac{5+z}{6}; \quad H_{31}(z) = \frac{1+5z}{6};$$

$$H_{51}(z) = \frac{z-1}{2T_i}; \quad H_{61}(z) = \frac{z-1}{2T_i};$$

$$H_{81}(z)=\frac{z-1}{T_i^2};\quad H_{91}(z)=\frac{1-z}{T_i^2};$$

$$H_{22}(z)=\frac{4-z}{6}T_i;\quad H_{32}(z)=\frac{1-4z}{6}T_i;$$

$$H_{52}(z)=-\frac{z}{2};\quad H_{62}(z)=-\frac{1}{2};$$

$$H_{82}(z)=-\frac{2+z}{T_i};\quad H_{92}(z)=\frac{1+2z}{T_i};$$

$$H_{23}(z)=\frac{2z+7}{36}T_i^2;\quad H_{33}(z)=\frac{2+7z}{36}T_i^2;$$

$$H_{53}(z)=\frac{1+2z}{12}T_i;\quad H_{63}(z)=-\frac{2+z}{12}T_i;$$

$$H_{83}(z)=\frac{2z-5}{6};\quad H_{93}(z)=\frac{2-5z}{6};$$

A.2. Analog reconstruction filters

Filters $h_0(x)$ and $h_1(x)$ are given again by (10) and (11), respectively.

$$h_2(x)=\frac{x^2}{4}-\frac{|x|^3}{6T_i}-\frac{|x|}{12}T_i \quad \text{para } |x|\leqslant T_i.$$

$$H_2(\Omega)=\left(\frac{2-\Omega^2T_i^2/6}{\Omega^4T_i}\cos(\Omega T_i)+\frac{1}{\Omega^3}\sin(\Omega T_i)\right.$$
$$\left.-\ \frac{2-\Omega^2T_i^2/6}{\Omega^4T_i}\right).$$

References

[1] V. Cherkassky, D. Gehring, F. Mulier, Comparison of adaptive methods for function estimation from samples, IEEE Trans. Neural Networks 7 (4) (1996) 969–984.

[2] A.M. Crosmun, S.A. Maas, Minimization of intermodulation distortion in GaAs MESFET small-signal amplifiers, IEEE Trans. Microwave Theory Tech. 37 (9) (1989) 1411–1417.

[3] I. Djokovic, P.P. Vaidyanathan, Generalized sampling theorems in multiresolution subspaces, IEEE Trans. Signal Process. 45 (3) (1997) 583–599.

[4] T. Fernández, Y. Newport, J.M. Zamanillo, A. Tazón, A. Mediavilla, Extracting a bias-dependent large signal MESFET model from I/V measurements, IEEE Trans. Microwave Theory Tech. 44 (3) (1996) 372–378.

[5] R.F. Hoskins, J.S. Pinto, Distributions, Ultradistributions and other Generalized Functions, Ellis Horwood, Chichester, 1994.

[6] A.J. Jerri, The Shannon sampling theorem—its various extension and applications: a tutorial review, Proc. IEEE 65 (11) (1977) 1565–1596.

[7] M. Lázaro, Técnicas de modelado no lineal con incorporación de restricciones en las derivadas y su aplicación a comunicaciones, Ph.D. Thesis, Universidad de Cantabria, Santander, Spain, 2001.

[8] M. Lázaro, I. Santamaría, C. Pantaleón, A regularized digital filtering technique for the simultaneous reconstruction of a function and its derivatives, in: Proceedings of the 8th International Conference on Electronics, Circuits and Systems (ICECS), Malta, 2001, pp. 67–70.

[9] D.A. Linden, A discussion of sampling theorems, Proc. IRE, Vol. 47, 1959, pp. 1219–1266.

[10] D.A. Linden, N.M. Abramson, A generalization of the sampling theorem, Inform. Control 3 (1960) 26–31.

[11] S.A. Maas, How to model intermodulation distortion, IEEE MTT-S International Microwave Symposium Digest, Boston, MA, USA, June 10–14, 1991, pp. 149–151.

[12] S.A. Maas, D. Neilson, Modeling MESFETs for intermodulation analysis of mixers and amplifiers, IEEE Trans. Microwave Theory Tech. 38 (12) (1990) 1964–1971.

[13] F. Marvasti, Advanced Topics in Shannon Sampling and Interpolation Theory, Springer, New York, 1993 (Ch. Nonuniform sampling).

[14] C. Navarro, A. Mediavilla, A. Tazón, Large signal dynamic properties of GaAs MESFET/HEMT devices under optical illumination, in: Proceedings of the GAAS'98 Symposium, Prague, Czech Republic, June 22–26, 1998, pp. 350–353.

[15] K.M. Perry, S.J. Reeves, A practical stopping rule for iterative signal restoration, in: Proceedings of the International Conference on Acoustics, Speech, and Signal Processing, Vol. III, Minneapolis (MI), 1993, pp. 440–443.

[16] H.N. Razafinjatovo, Iterative reconstructions in irregular sampling with derivatives, J. Fourier Anal. Appl. 1 (3) (1995) 281–295.

[17] S.J. Reeves, R.M. Mersereau, Optimal estimation of the regularization parameters and stabilizing functional for regularized image restoration, Opt. Eng. 29 (5) (1990) 446–454.

[18] C.E. Shannon, Communications in the presence of noise, Proc. IRE, Vol. 37, 1949, pp. 10–21.

[19] M. Unser, A. Aldroubri, M. Eden, B-spline signal processing: Part I - theory, IEEE Trans. Signal Process. 41 (2) (1993) 821–833.

[20] P.P. Vaidyanathan, B. Vrcelj, On sampling theorems for non bandlimited signals, in: Proceedings of the International Conference on Acoustics, Speech, and Signal Proccesing, Vol. 6, Salt Lake City, UT, USA, May 8–11, 2001, pp. 3897–3900.

[21] J.M. Whittaker, Interpolatory Function Theory, Cambridge University Press, Cambridge, 1935.